Topography of the graphene/Ir(111) moiré studied by surface x-ray diffraction

Fabien Jean,[1,2,*] Tao Zhou,[1,3] Nils Blanc,[1,2] Roberto Felici,[4] Johann Coraux,[1,2] and Gilles Renaud[1,3]

[1]*Univ. Grenoble Alpes, F-38000 Grenoble, France*

[2]*CNRS, Inst NEEL, F-38042 Grenoble, France*

[3]*CEA, INAC-SP2M, Grenoble, F-38054, France*

[4]*European Synchrotron Radiation Facility, Boîte Postale 220, F-38043 Grenoble Cedex 9, France*

The structure of a graphene monolayer on Ir(111) has been investigated *in situ* in the growth chamber by surface x-ray diffraction including the specular rod, which allows disentangling the effect of the sample roughness from that of the nanorippling of graphene and iridium along the moiré-like pattern between graphene and Ir(111). Accordingly, we are able to provide precise estimates of the undulation associated with this nanorippling, which is small in this weakly interacting graphene-metal system and thus has proved difficult to assess in the past. The nanoripplings of graphene and iridium are found in phase, i.e., the in-plane positions of their height maxima coincide, but the amplitude of the height modulation is much larger for graphene (0.379 ± 0.044 Å) than, e.g., for the topmost Ir layer (0.017 ± 0.002 Å). The average graphene-Ir distance is found to be 3.38 ± 0.04 Å.

I. INTRODUCTION

Graphene, a monoatomic layer of carbon atoms arranged in a honeycomb lattice, has been investigated thoroughly in the past 10 years because of its exceptional properties, which hold promise for numerous applications [1]. Transition-metal surfaces form a broad family of substrates for the growth of large-area, high-quality graphene [2]. New properties can be induced in graphene through the interaction with the substrate, e.g., electronic band gaps [3], spin polarization [4], and superconductivity [5]. In most graphene-on-metal systems, the interaction is modulated at the nanoscale due to lattice mismatch between graphene and the metal, which results in two-dimensional patterns with periodicity of the order of nanometers, often referred to as moirés, following an analogy with the beating of optical waves through two mismatched periodic lattices (e.g., tissue veils). Knowledge of the topographic properties of these moirés, i.e., the average graphene-metal distance, and the perpendicular-to-the-surface amplitude of the graphene and metal undulations across the moiré is desirable in view of characterizing the interaction and rationalizing the other properties.

The topography is, however, hard to grasp at such small scales. Most efforts that have relied on scanning tunneling microscopy have faced the issue of the entanglement of the structural and local density of states which is inherent in the tunneling effect. A striking illustration has been the debate on the amplitude [6,7] and sign [8,9] of the moiré-related undulation in graphene/Ru(0001) and graphene/Ir(111), respectively. Atomic force microscopy (AFM) has proven to be a valuable alternative, provided it is performed with care, especially with respect to the possible chemical interaction between the tip and sample [10,11]. Scattering techniques, such as low-energy electron diffraction (LEED), surface x-ray diffraction (SXRD), and x-ray standing waves (XSW), are free of such probe-induced perturbations of the systems. At the expense of complex calculations in the framework of the dynamical theory of diffraction, LEED was used to assess the topography of graphene/Ru(0001) [12] and graphene/Ir(111) [11]. SXRD was used to analyze the topography of graphene/Ru(0001) [13], and XSW was used to analyze the topography of graphene/Ir(111) [8]. Confirming and refining the results obtained with these approaches is of prime importance in order to set reliable points of reference for first-principles calculations, which are cumbersome in essence in such systems due to the importance of nonlocal (e.g., van der Waals) interactions [14].

Here, we address the model graphene/Ir(111) system, typical of a weak graphene-metal interaction. Its moiré topography deviates only slightly from the flat case and is thus difficult to characterize. With the help of two techniques, SXRD and extended x-ray reflectivity (EXRR), the latter of which has not been employed to characterize monolayer graphene on a substrate before, we deduce an average 3.38 ± 0.04 Å distance between graphene and Ir(111) and determine, with an uncertainty as low as that of scanning probe microscopy [11], a 0.379 ± 0.044 Å amplitude of the graphene undulation. In addition, we are able to estimate the undulation of the Ir layers, which is usually not accessible in other techniques, and find 0.017 ± 0.002 Å for the topmost one.

II. EXPERIMENTAL METHODS

The synchrotron x-ray diffraction measurements were performed in ultrahigh-vacuum chambers coupled with z-axis diffractometers at the BM32 and ID03 beam lines of the European Synchrotron Radiation Facility. Details on the chambers and the beam are given in Ref [15]. The nonspecular crystal truncation rods (CTRs) were measured on BM32, and the specular rod, 00L, was measured by EXRR on ID03. The x-ray beam energy was set at 11 keV. The reciprocal-space scans of the scattered intensity presented below are all normalized to the intensity measured with a monitor placed before the sample. For the SXRD measurements, the intensity along the Ir(111) CTRs and along the graphene rods was measured with a Maxipix two-dimensional detector in stationary mode for the upper range of the out-of-plane scattering vector

*fabien.jean@neel.cnrs.fr

component (i.e., large values of the out-of-plane reciprocal-space coordinate L) and by performing sample rocking scans for low L values [16]. The amplitude of the structure factors $F_{H,K}(L)$, the square root of the measured intensity, for the different CTRs and graphene rods, each corresponding to different values of the in-plane reciprocal-space parameters H and K, was extracted and processed with the PYROD program described in Ref. [16]. PYROD was also used to simulate the structure factors using the model described below and to refine the structural parameters of this model with the help of a least-squares fit of the simulation to the data. The total uncertainty of the experimental structure factors is dominated by the systematic error, which is estimated to be 6.1%, according to Ref. [16]; the statistical error is everywhere smaller than 1%.

The Ir single crystals were cleaned according to a procedure described in Ref. [15] that allows for considerably reducing the concentration of residual carbon in bulk Ir(111). Graphene was grown in two steps, first by 1473 K annealing of a room-temperature-adsorbed monolayer of ethylene and second by exposure to 10^{-8} mbar of ethylene with the surface held at 1273 K. This growth procedure, temperature programed growth (TPG), allows for selecting a well-defined crystallographic orientation of purely single-layer graphene with respect to Ir(111) [17]. Compared to the samples studied in Refs. [8,11], the surface coverage is larger (100%) in our case. Our growth procedure is similar to that used to prepare the 100%-coverage graphene studied in Ref. [18], yet the temperatures which we chose for each step are different and are actually identical to those used for preparing one of the samples addressed in Ref. [15]. We note that both the graphene coverage and growth temperature have been
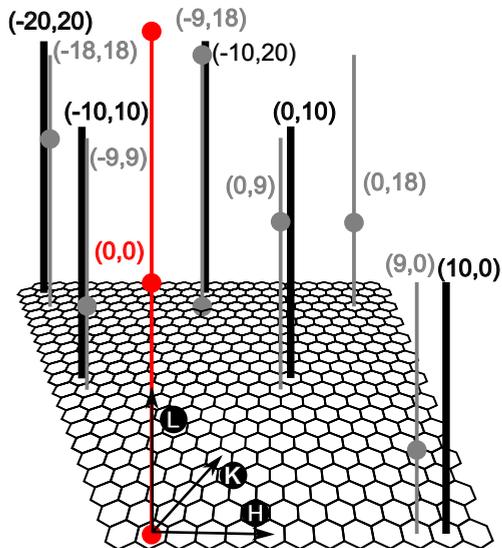
argued to influence the structure of graphene [8,19] and thus its properties [20]. Two samples were prepared, one in each of the UHV chambers installed at the BM32 and ID03 beam lines, where the SXRD and EXRR experiments were performed, respectively. The hexagonal lattice unit cell of the iridium surface has a lattice parameter of 2.7147 Å at room temperature. The graphene unit cell has a measured lattice parameter of 2.4530 Å. The ratio between the two lattice parameters, 0.903, is close to 0.9. Therefore, in the following we assume that the system is commensurate with a (10×10) graphene cell coinciding with a (9×9) iridium one. In the following, the in-plane unit cell of reciprocal space is the moiré one [21]. This corresponds to H and K indexes in multiples of 9 and 10 for Ir CTRs and graphene rods, respectively (Fig. 1).

III. RESULTS AND ANALYSIS

Figure 2 shows the Ir CTRs and graphene rods. As expected for an (essentially) two-dimensional layer such as graphene, the graphene rods are basically featureless [22]. Qualitatively,

FIG. 1. (Color online) Sketch of the reciprocal space. The hexagonal grid shows the partition of its (H,K) plane according to the 10-on-9 commensurability. H, K, and L are in reciprocal lattice units of the moiré (superlattice) surface unit cell. The measured CTRs from the iridium are shown in gray, with circles to highlight the positions of the different Bragg reflections. The graphene rods are shown in black. The specular CTR ($H = K = 0$) is shown in red. Each is labeled with its (H,K) position in the 10-on-9 moiré surface supercell.
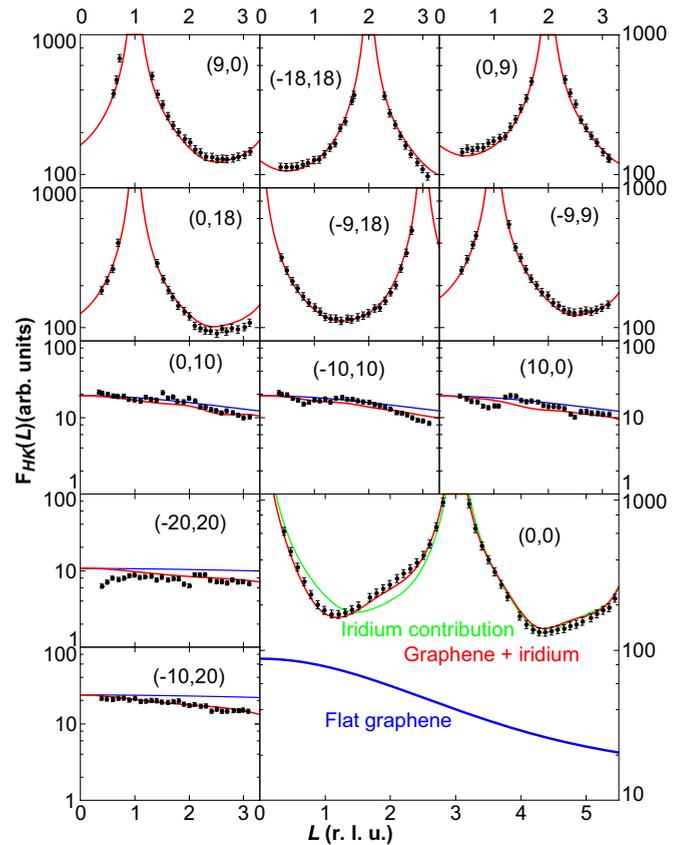
FIG. 2. (Color online) Experimental structure factors $F_{H,K}(L)$ of iridium CTRs and graphene rods from SXRD measurements of the first sample (in black with the error bars). The solid red lines represent the best fit with the Fourier model. The contribution of a flat graphene layer alone is shown in blue to highlight the effect of the rugosity and undulations on the rods. The specular rod (0,0) from the second sample is reported in the bottom right in black with error bars. The solid red line represents the final fit, the green one shows the contribution of the iridium alone, and the blue line shows the contribution of a flat graphene layer alone.
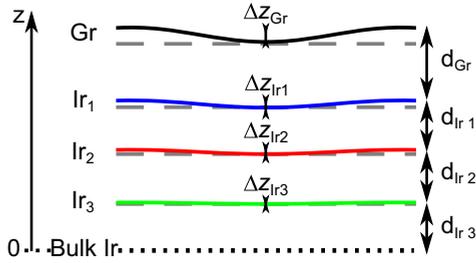
FIG. 3. (Color online) Sketch of the parameters studied. The black line is the graphene, and the blue, red, and green lines are the surface layers of iridium. The amplitudes of their corrugation are shown by arrows in the middle. The start of the bulk iridium is sketched with the dotted black line. The gray dashed lines represents the expected bulk positions for the different atomic layers without corrugation. The z axis on the left is a reference to the linear dependency of the iridium corrugation amplitude.

because the undulations of the graphene and top substrate layers are expected to be small, the main features are (i) the pronounced interference effect on the specular rod $F_{0,0}(L)$ related to the average distance dz_{Gr} between Ir and graphene, which is expected to be larger than the bulk distance of 2.2 Å, (ii) the decrease of the otherwise featureless CTRs in between Bragg peaks, related to the substrate roughness, and (iii) the decrease of the graphene rods with increasing L, dominated by the undulation of the graphene layer, as shown by the simulated graphene rods for a flat graphene layer alone in Fig. 2. This decorrelation between roughness and undulation allows these parameters to be determined with high accuracy.

In order to achieve a quantitative characterization of the topography of the system, we introduce a simple model [23]. A limited set of parameters (see Fig. 3), including the average interplanar distances, the actual roughness, and the amplitude of undulation of each layer, seems to be a reasonable option for a simple modeling of the system. In order to approach this description, we introduce a lattice model based on a Fourier series, such as the one proposed for graphene/Ru(0001) [24]. In this model, the displacement in the direction i ($i = \{x,y,z\}$) of an atom with x, xy, and z coordinates with respect to the corresponding position in a flat layer is given by

$$dr^i = \sum_{s,t} A^i_{s,t}\sin[2\pi(sx+ty)] + B^i_{s,t}\cos[2\pi(sx+ty)],$$

(1)

where the sum runs over the different orders of the series. Due to the crystal symmetry of graphene and Ir(111), the displacements must respect a $p3m1$ symmetry; that is, they

must fulfill

$$R_j^{-1}\{d\mathbf{r}[R_j(\mathbf{r})]\} = R_j\{d\mathbf{r}[R_j^{-1}(\mathbf{r})]\},$$

(2)

with $j \in [0,5]$. R_0 is the identity matrix, R_1 and R_2 correspond to the $\pm 120°$ rotations, and the last three correspond to the mirror planes.

$$R_0 = \begin{pmatrix} 1 & 0 \\ 0 & 1 \end{pmatrix}, \quad R_1 = \begin{pmatrix} 0 & \bar{1} \\ 1 & \bar{1} \end{pmatrix}, \quad R_2 = \begin{pmatrix} \bar{1} & 1 \\ \bar{1} & 0 \end{pmatrix},$$

$$R_3 = \begin{pmatrix} 0 & \bar{1} \\ \bar{1} & 0 \end{pmatrix}, \quad R_4 = \begin{pmatrix} \bar{1} & 1 \\ 0 & 1 \end{pmatrix}, \quad R_5 = \begin{pmatrix} 1 & 0 \\ 1 & \bar{1} \end{pmatrix}.$$

(3)

These symmetry constraints impose the condition that not all Fourier coefficients in Eq. (1) are independent. Their relationships are given in Table I.

In the following we further simplify the model by limiting the Fourier development to first order, which is legitimate because no significant diffraction data are measurable beyond first order (a diffraction experiment is actually a measurement of the Fourier transform of the electronic density and thus, to a good approximation, of the shape of graphene). Also, we assume that the undulations of all Ir layers are in phase, as found in density functional theory (DFT) calculations. In this framework, the x, xy, and z displacements are simply written as

$$dr^x = A^x\{2\sin(2\pi x) + \sin(2\pi y) + \sin[2\pi(x-y)]\}$$
$$+ B^x\{2\cos(2\pi x) - \cos(2\pi y) - \cos[2\pi(x-y)]\},$$

(4)

$$dr^y = A^x\{\sin(2\pi x) + 2\sin(2\pi y) - \sin[2\pi(x-y)]\}$$
$$+ B^x\{\cos(2\pi x) - 2\cos(2\pi y) + \cos[2\pi(x-y)]\},$$

(5)

$$dr^z = A^z\{2\sin(2\pi x) - 2\sin(2\pi y) - 2\sin[2\pi(x-y)]\}$$
$$+ B^z\{2\cos(2\pi x) + 2\cos(2\pi y) + 2\cos[2\pi(x-y)]\}.$$

(6)

Thus, only two variables per atomic plane, A^x and B^x, are needed to describe the in-plane displacements. The model is applied to graphene/Ir(111), with three iridium layers and one graphene layer. Each of these layers is characterized by four Fourier coefficients (A^x, B^x, A^z, and B^z), plus another parameter corresponding to an average z displacement of the layer from its equilibrium position in the bulk. This distance between metal planes parallel to the surface is known to vary, in some cases by as much as a few percent and in a nonmonotonous manner across the few topmost layers of metal surfaces [25]. In order to reduce the number of free

TABLE I. Relationships between the Fourier coefficients $A^i_{s,t}$ and $B^i_{s,t}$ ($i = \{x,y,z\}$).

$$A^x_{s,t} = -A^x_{t,-s-t} + A^y_{t,-s-t} = -A^y_{-s-t,s} = -A^y_{-t,-s} = -A^x_{-s,s+t} + A^y_{-s,s+t} = A^x_{s+t,-t}$$

$$A^y_{s,t} = A^x_{-s-t,s} - A^y_{-s-t,s} = -A^x_{t,-s-t} = -A^x_{-t,-s} = -A^y_{-s,s+t} = A^x_{s+t,-t} - A^y_{s+t,-t}$$

$$A^z_{s,t} = A^z_{t,-s-t} = A^z_{-s-t,s} = A^z_{-t,-s} = A^z_{-s,s+t} = A^z_{s+t,-t}$$

$$B^x_{s,t} = -B^x_{t,-s-t} + B^y_{t,-s-t} = -B^y_{-s-t,s} = -B^y_{-t,-s} = -B^x_{-s,s+t} + B^y_{-s,s+t} = B^x_{s+t,-t}$$

$$B^y_{s,t} = B^x_{-s-t,s} - B^y_{-s-t,s} = -B^x_{t,-s-t} = -B^x_{-t,-s} = -B^y_{-s,s+t} = B^x_{s+t,-t} - B^y_{s+t,-t}$$

$$B^z_{s,t} = B^z_{t,-s-t} = B^z_{-s-t,s} = B^z_{-t,-s} = B^z_{-s,s+t} = B^z_{s+t,-t}$$

TABLE II. Topographic parameters for the two samples, the DFT calculations data from Ref. [8], and results from Ref. [8] (XSW) and [11] (LEED + AFM). dz_{Gr} is the mean distance between the graphene and its substrate. Δz_{Gr} is the graphene undulation amplitude. dz_{Ir_1}, dz_{Ir_2}, and dz_{Ir_3} are the interlayer distances of the iridium surface layers, and Δz_{Ir_1}, Δz_{Ir_1}, and Δz_{Ir_1} are their undulation amplitudes. ρ is the roughness of the sample surface, and O_{Gr} is the graphene coverage.

	SXRD (first sample)	EXRR (second sample)	DFT calculations	Busse et al. [8]	Hämäläinen et al. [11]
dz_{Gr} (Å)	3.39 ± 0.28	3.38 ± 0.04	3.43	3.38 ± 0.04	3.39 ± 0.03
Δz_{Gr} (Å)	0.379 ± 0.044		0.46	0.6 ± 0.1 1.0 ± 0.2	0.47 ± 0.05
dz_{Ir_1} (Å)	2.203 ± 0.012	2.203 ± 0.010	2.190		2.222
dz_{Ir_2} (Å)	2.212 ± 0.007	2.205 ± 0.008	2.175		2.224
dz_{Ir_3} (Å)	2.223 ± 0.002	2.225 ± 0.004	2.184		2.222
Δz_{Ir_1} (Å)	0.017 ± 0.002		0.015		0.006
Δz_{Ir_2} (Å)	0.011 ± 0.001		0.012		0.006
Δz_{Ir_3} (Å)	0.006 ± 0.001		0.004		0
ρ (Å)	0.42 ± 0.20	1.05 ± 0.08			
O_{Gr} (%)	98 ± 2	89.7 ± 1	100	39 63	Partial

parameters, however, we assume a linear dependence of the distance between Ir(111) planes, and thus of A^z and B^z, as a function of depth. This assumption complies with the results of the DFT simulations (see Table II), where the topographic parameters of the model are listed.

The Fourier model was used to fit the SXRD data. The expected in-plane displacements, which are below 0.01 Å according to first-principles calculations [8], have no noticeable influence on the Ir CTRs and graphene rods and are discarded in the simulations [26]. The best fit lead to a χ^2 value of 3.5 and the results are shown in Table II and Fig. 4. We find 98% $\pm$ 2% graphene coverage. Graphene is found to have a mean distance of $dz_{Gr} = 3.39 \pm 0.28$ Å from its substrate and a corrugation of $\Delta z_{Gr} = 0.379 \pm 0.044$ Å. The graphene distance from its substrate is close to the interlayer spacing in graphite, 3.36 Å. As explained above, the benefit of the SXRD analysis of both graphene and Ir contributions, as compared to other techniques, is to provide an accurate value of the amplitude of the graphene undulation perpendicular to the surface. The interlayer Ir spacings are found to be 2.203 ± 0.012, 2.212 ± 0.007, and 2.223 ± 0.002 Å from top to bottom. The topmost layer of iridium has an undulation of 0.017 ± 0.002 Å, the second layer has an undulation of 0.011 ± 0.001 Å, and the last one is 0.006 ± 0.001 Å. Finally, the roughness of the

iridium substrate is found to be 0.42 ± 0.20 Å, following a simple β model [27]. This small value may be linked to the small coherence length of the x-ray beam (corresponding to about ten flat Ir terraces separated by atomic step edges) on the BM32 beam line.

IV. DISCUSSION

The best fit between simulations and SXRD data is achieved for an iridium undulation in phase with the graphene one, with a smaller amplitude, however. This finding is at variance with that obtained in earlier scanning probe microscopy measurements performed in specific imaging conditions [9] and supports the picture progressively assembled through other reports based on scanning probe microscopies [10,28], XSW [8], and first-principles calculations [8,29].

The main limitation of this SXRD analysis is the rather large uncertainty of the dz_{Gr} distance. This motivated complementary measurements of the specular rod in the second sample, using the ID03 setup as the extended reflectivity was not accessible in the BM32 setup. The EXRR result is shown in Fig. 2 together with the best fit and simulated and graphene specular rods. The best fit of the specular rod, yielding a χ^2 value of 1.064, was done with a simplified model in which the undulations of both the iridium and graphene were fixed at the values obtained from the SXRD analysis. It yields a value of $dz_{Gr} = 3.38$ Å, very close to that determined in the other sampler by off-specular SXRD but with a much better accuracy, ± 0.04 Å. The graphene layer of this second sample is found to be incomplete, with a 90% $\pm$ 2% graphene coverage. In addition, the spacings between the topmost Ir planes are found to be 2.203 ± 0.010, 2.205 ± 0.008, and 2.225 ± 0.004 Å from top to bottom (2.217 Å in the bulk). We find interlayer distances between Ir(111) planes that are larger than those found in the absence of graphene [30]. This finding is consistent with the p doping found for graphene [3], which implies electron transfers from graphene to Ir(111). The corresponding higher electronic density in Ir(111) is expected
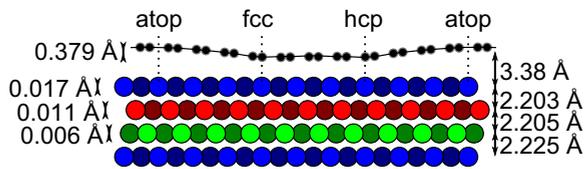

FIG. 4. (Color online) Cut of the 10-on-9 commensurability to represent the corrugations and displacements of the atomic layers. Carbon atoms of the graphene are black circles; the iridium atoms are in blue, red, and green to show the ABC stacking of the different layers. The three coincidence regions of graphene with the substrate and the corrugations and interlayer spacing are denoted.
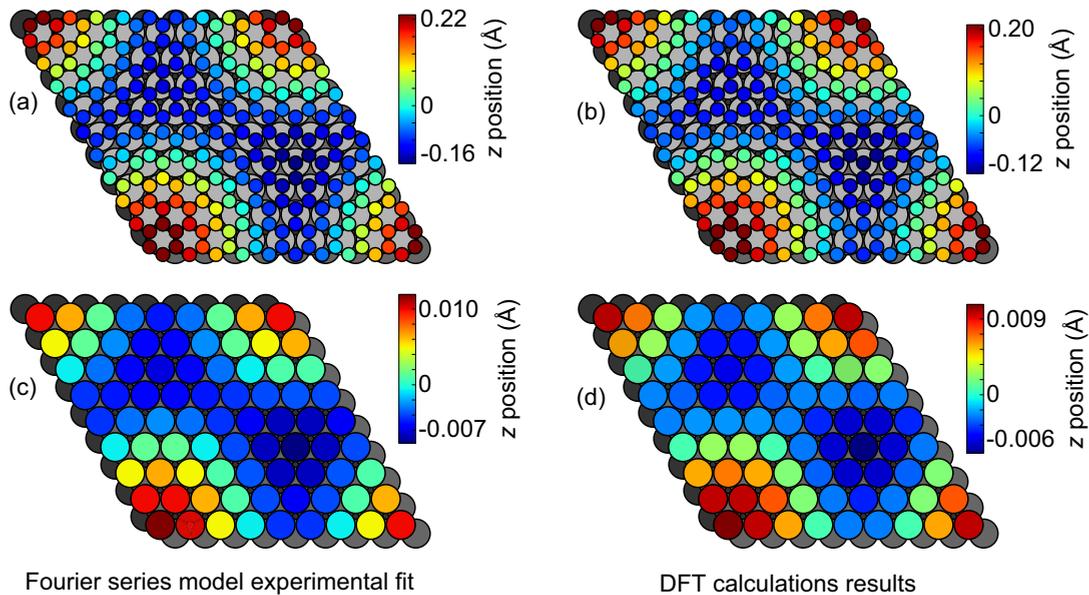
FIG. 5. (Color online) Sketches of the graphene out-of-plane variations from (a) the Fourier model used on the experimental data and (b) the DFT calculation results and the out-of-plane variations of the topmost iridium layer from (c) the Fourier model used on the experimental data and (d) the DFT calculation results. The out-of-plane corrugation is shown with a color gradient, with the scales in amperes.

to counterbalance the surface relaxation in bare Ir(111). The substrate roughness in this case is found to be $1.1 \pm 0.1\,\text{Å}$, which is larger than that obtained from SXRD. This is, however, expected since the coherence length of the beam is two orders of magnitude larger here; for example, around 1000 atomic steps of the substrate scatter the beam coherently.

Because the sample in this study has complete graphene coverage, the deviations from previous studies can be explained by strains in the full layer that can relax in the graphene island. These deviations could also be explained by the differences in the growth process (temperature, methods, etc.), and Busse *et al.* [8] showed that the undulation varies depending on the graphene coverage. Moreover, the undulation could also be affected by the growth methods (full/partial growth, chemical vapor deposition, temperature-programed growth, etc.) and growth temperature because it has been reported that these parameters affect the graphene lattice parameter and its commensurability with the substrate [15,19]. The iridium undulations are also found to be larger than those deduced from a LEED study [11]. This difference might be due to some limitation of LEED to analyze layers below the graphene one because of the small electron mean free path.

The graphene-metal distance which we obtain is in good agreement with values deduced by XSW, LEED, and AFM (see Table II). The undulation of the graphene which we obtain is also in agreement with that found by LEED and AFM. It is, however, smaller than that deduced from XSW. The difference might originate from two effects. First, we recently found that the in-plane lattice parameter of graphene varies as a function of the preparation method, which is different in Refs. [8,11] (several TPG cycles at 1420 K for different coverages and one TPG at 1500 K, respectively) and in the present work (TPG at 1473 K followed by chemical vapor deposition at 1273 K for complete coverage). Given that the strain is closely related to the graphene buckling (undulation) [18], we indeed expect

different undulations in each of these reports. Second, the strain (and thus buckling) of graphene was argued to depend on the fraction of edge atoms in graphene, i.e., on graphene coverage [8]. Our results, unlike those in Refs. [8,11], address close-to-full layer graphene.

The Fourier model was also tested to fit the displacements obtained by the DFT calculations described in Ref. [8]. The model was in very good agreement with the DFT calculation results, particularly the iridium top layer and graphene, thus confirming that the first-order Fourier component is enough to describe the system, as shown in Fig. 5. Moreover, it also confirmed that A^z and B^z of the three iridium layers have an almost linear dependence as a function of depth. From the DFT simulation, the corrugations of the iridium surface layers from top to bottom are 0.015, 0.012, and 0.04 Å, while that of the graphene is 0.35 Å, which is close to the experimental results.

In fact, this analysis has a limit too, as our starting hypothesis on the structure of the supercell, a (10×10) graphene cell coinciding with a (9×9) iridium, may have an impact on the results. It was reported previously that this system cannot be consider fully commensurate as it is really a composition of commensurate domains with incommensurate boundaries [19] and that the thermal history of the sample affects it [15,19]. Here, the 9.03 ratio indicates that there should be a combination of $(10 \times 10)/(9 \times 9)$, $(21 \times 21)/(19 \times 19)$, and incommensurate domains. However, despite the complexity of the sample, the starting hypothesis of the problem allows us to extract a good approximation of the actual structure.

V. CONCLUSION

To conclude, we have employed SXRD to determine with high resolution, on the basis of a simple structural model, the structure of a weakly scattering atomically thin membrane (graphene) weakly interacting with a metallic substrate made

of strong scatterers (Ir atoms). We determine the undulation of graphene across the moiré-like superstructure formed between graphene and Ir(111), 0.379 ± 0.044, without the ambiguity inherent in other ensemble-averaging techniques. Our determination of the average graphene-Ir(111) distance is consistent with previous reports based on local-probe and ensemble-averaging analysis. Finally, we unveil the faint corrugations predicted by DFT calculations in the substrate, which are as low as 0.017 ± 0.002 for the topmost Ir layer and are characteristic of a weak C-Ir bonding with a slight covalent character in some of the sites of the moiré. The use of SXRD for other two-dimensional membranes, such as transition-metal dichalcogenides, boron nitride, and monolayer silica, should allow for constructing a comprehensive picture of the nanomechanics of atomically thin membranes under the influence of substrates.

[1] K. S. Novoselov, V. I. Fal'ko, L. Colombo, P. R. Gellert, M. G. Schwab, and K. Kim, Nature (London) **490**, 192 (2012).

[2] H. Tetlow, J. De Boer, I. Ford, D. Vvedensky, J. Coraux, and L. Kantorovich, Phys. Rep. **542**, 195 (2014).

[3] I. Pletikosić, M. Kralj, P. Pervan, R. Brako, J. Coraux, A. T. N'Diaye, C. Busse, and T. Michely, Phys. Rev. Lett. **102**, 056808 (2009).

[4] A. Varykhalov, J. Sánchez-Barriga, A. M. Shikin, C. Biswas, E. Vescovo, A. Rybkin, D. Marchenko, and O. Rader, Phys. Rev. Lett. **101**, 157601 (2008).

[5] C. Tonnoir, A. Kimouche, J. Coraux, L. Magaud, B. Delsol, B. Gilles, and C. Chapelier, Phys. Rev. Lett. **111**, 246805 (2013).

[6] S. Marchini, S. Günther, and J. Wintterlin, Phys. Rev. B **76**, 075429 (2007).

[7] A. L. Vázquez De Parga, F. Calleja, B. Borca, M. C. G. Passeggi, Jr., J. J. Hinarejos, F. Guinea, and R. Miranda, Phys. Rev. Lett. **100**, 056807 (2008).

[8] C. Busse, P. Lazić, R. Djemour, J. Coraux, T. Gerber, N. Atodiresei, V. Caciuc, R. Brako, S. Blügel, J. Zegenhagen, and T. Michely, Phys. Rev. Lett. **107**, 036101 (2011).

[9] Z. Sun, S. K. Hämäläinen, J. Sainio, J. Lahtinen, D. Vanmaekelbergh, and P. Liljeroth, Phys. Rev. B **83**, 081415 (2011).

[10] Y. Dedkov and E. Voloshina, Phys. Chem. Chem. Phys. **16**, 3894 (2014).

[11] S. K. Hämäläinen, M. P. Boneschanscher, P. H. Jacobse, I. Swart, K. Pussi, W. Moritz, J. Lahtinen, P. Liljeroth, and J. Sainio, Phys. Rev. B **88**, 201406 (2013).

[12] W. Moritz, B. Wang, M.-L. Bocquet, T. Brugger, T. Greber, J. Wintterlin, and S. Günther, Phys. Rev. Lett. **104**, 136102 (2010).

[13] D. Martoccia, P. Willmott, T. Brugger, M. Björck, S. Günther, C. Schlepütz, A. Cervellino, S. Pauli, B. Patterson, S. Marchini *et al.*, Phys. Rev. Lett. **101**, 126102 (2008).

[14] F. Mittendorfer, A. Garhofer, J. Redinger, J. Klimeš, J. Harl, and G. Kresse, Phys. Rev. B **84**, 201401 (2011).

[15] F. Jean, T. Zhou, N. Blanc, R. Felici, J. Coraux, and G. Renaud, Phys. Rev. B **88**, 165406 (2013).

[16] J. Drnec, T. Zhou, S. Pintea, W. Onderwaater, E. Vlieg, G. Renaud, and R. Felici, J. Appl. Crystallogr. **47**, 365 (2014).

[17] R. Van Gastel, A. N'Diaye, D. Wall, J. Coraux, C. Busse, N. Buckanie, F.-J. Meyer Zu Heringdorf, M. Horn Von Hoegen, T. Michely, and B. Poelsema, Appl. Phys. Lett. **95**, 121901 (2009).

[18] S. Runte, P. Lazić, C. Vo-Van, J. Coraux, J. Zegenhagen, and C. Busse, Phys. Rev. B **89**, 155427 (2014).

[19] N. Blanc, J. Coraux, C. Vo-Van, O. Geaymond, and G. Renaud, Phys. Rev. B **86**, 235439 (2012).

[20] D. Usachov, A. Fedorov, O. Vilkov, V. K. Adamchuk, L. V. Yashina, L. Bondarenko, A. A. Saranin, A. Grüneis, and D. V. Vyalikh, Phys. Rev. B **86**, 155151 (2012).

[21] J. Coraux, A. N'Diaye, C. Busse, and T. Michely, Nano Lett. **8**, 565 (2008).

[22] A. Charrier, A. Coati, T. Argunova, F. Thibaudau, Y. Garreau, R. Pinchaux, I. Forbeaux, J.-M. Debever, M. Sauvage-Simkin, and J.-M. Themlin, J. Appl. Phys. **92**, 2479 (2002).

[23] Independently refining the positions of each atom in a commensurate cell, comprising a few hundred C and Ir atoms, obviously would provide an unreliable structural picture given that the number of free parameters would approach or even exceed the number of experimental points.

[24] D. Martoccia, M. Björck, C. Schlepütz, T. Brugger, S. Pauli, B. Patterson, T. Greber, and P. Willmott, New J. Phys. **12**, 043028 (2010).

[25] D. Adams, L. Petersen, and C. Sorensen, J. Phys. C **18**, 1753 (1985).

[26] Actually, we tested that even 0.05-Å in-plane displacements have no substantial effect.

[27] I. K. Robinson, Phys. Rev. B **33**, 3830 (1986).

[28] M. Boneschanscher, J. van der Lit, Z. Sun, I. Swart, P. Liljeroth, and D. Vanmaekelbergh, ACS Nano **6**, 10216 (2012).

[29] A. T. N'Diaye, S. Bleikamp, P. J. Feibelman, and T. Michely, Phys. Rev. Lett. **97**, 215501 (2006).

[30] Y. He, A. Stierle, W. Li, A. Farkas, N. Kasper, and H. Over, J. Phys. Chem. C **112**, 11946 (2008).